

**AFRL-PR-WP-TR-2001-2035**

**EMBEDDED HEAT PIPES IN CERAMIC  
ELECTRONIC PACKAGES AND FILLING  
PROCESS**



**K. JONES  
Y. CAO  
M. GAO**

**Florida International University  
Department of Mechanical Engineering  
EAS 3462 University Park  
Miami, Florida 33199**

**FEBRUARY 2001**

**FINAL REPORT FOR PERIOD 01 JANUARY 1997 – 31 DECEMBER 2000**

**Approved for public release; distribution unlimited.**

**20020617 126**

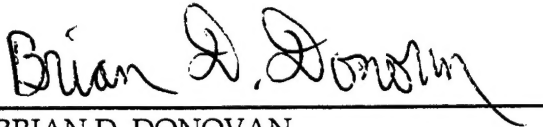
**PROPULSION DIRECTORATE  
AIR FORCE RESEARCH LABORATORY  
AIR FORCE MATERIEL COMMAND  
WRIGHT-PATTERSON AIR FORCE BASE, OH 45433-7251**

## NOTICE

USING GOVERNMENT DRAWINGS, SPECIFICATIONS, OR OTHER DATA INCLUDED IN THIS DOCUMENT FOR ANY PURPOSE OTHER THAN GOVERNMENT PROCUREMENT DOES NOT IN ANY WAY OBLIGATE THE US GOVERNMENT. THE FACT THAT THE GOVERNMENT FORMULATED OR SUPPLIED THE DRAWINGS, SPECIFICATIONS, OR OTHER DATA DOES NOT LICENSE THE HOLDER OR ANY OTHER PERSON OR CORPORATION; OR CONVEY ANY RIGHTS OR PERMISSION TO MANUFACTURE, USE, OR SELL ANY PATENTED INVENTION THAT MAY RELATE TO THEM.

THIS REPORT IS RELEASABLE TO THE NATIONAL TECHNICAL INFORMATION SERVICE (NTIS). AT NTIS, IT WILL BE AVAILABLE TO THE GENERAL PUBLIC, INCLUDING FOREIGN NATIONS.

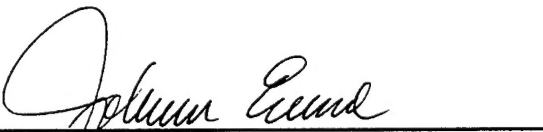
THIS TECHNICAL REPORT HAS BEEN REVIEWED AND IS APPROVED FOR PUBLICATION.



BRIAN D. DONOVAN  
Mechanical Engineer  
Energy Storage & Thermal Sciences Branch



BRIAN G. HAGER  
Chief  
Energy Storage & Thermal Sciences Branch



JOANN L. ERNO, Lt Col, USAF  
Deputy Chief  
Power Division

Do not return copies of this report unless contractual obligations or notice on a specific document requires its return.

# REPORT DOCUMENTATION PAGE

Form Approved  
OMB No. 0704-0188

The public reporting burden for this collection of information is estimated to average 1 hour per response, including the time for reviewing instructions, searching existing data sources, gathering and maintaining the data needed, and completing and reviewing the collection of information. Send comments regarding this burden estimate or any other aspect of this collection of information, including suggestions for reducing this burden, to Department of Defense, Washington Headquarters Services, Directorate for Information Operations and Reports (0704-0188), 1215 Jefferson Davis Highway, Suite 1204, Arlington, VA 22202-4302. Respondents should be aware that notwithstanding any other provision of law, no person shall be subject to any penalty for failing to comply with a collection of information if it does not display a currently valid OMB control number. PLEASE DO NOT RETURN YOUR FORM TO THE ABOVE ADDRESS.

1. REPORT DATE (DD-MM-YY) February 2001		2. REPORT TYPE Final		3. DATES COVERED (From - To) 01/01/1997 - 12/31/2000	
4. TITLE AND SUBTITLE Embedded Heat Pipes In Ceramic Electronic Packages And Filling Process				5a. CONTRACT NUMBER F33615-96-C-2659	
				5b. GRANT NUMBER	
				5c. PROGRAM ELEMENT NUMBER 62173C	
6. AUTHOR(S) K. Jones Y. Cao M. Gao				5d. PROJECT NUMBER 1651	
				5e. TASK NUMBER 01	
				5f. WORK UNIT NUMBER 05	
7. PERFORMING ORGANIZATION NAME(S) AND ADDRESS(ES) Florida International University Department of Mechanical Engineering EAS 3462 University Park Miami, Florida 33199				8. PERFORMING ORGANIZATION REPORT NUMBER	
9. SPONSORING/MONITORING AGENCY NAME(S) AND ADDRESS(ES) PROPULSION DIRECTORATE AIR FORCE RESEARCH LABORATORY AIR FORCE MATERIEL COMMAND WRIGHT-PATTERSON AIR FORCE BASE, OH 45433-7251				10. SPONSORING/MONITORING AGENCY ACRONYM(S) AFRL/PRPS	
				11. SPONSORING/MONITORING AGENCY REPORT NUMBER(S) AFRL-PR-WP-TR-2001-2035	
12. DISTRIBUTION/AVAILABILITY STATEMENT Approved for public release; distribution unlimited.					
13. SUPPLEMENTARY NOTES					
14. ABSTRACT The development of a new technology for electronic cooling is described in this report. By integrating heat pipes directly within the ceramic substrate, effective thermal conduction for spreading heat in both radial and axial directions was achieved. Several prototype miniature heat pipes have been fabricated in HTCC and LTCC substrates in the Hybrid Lab at FIU using numerically controlled machining operations. The heat pipes use an axially grooved wick structure to facilitate transport of the working fluid from the condenser to the evaporator. Three liquid charging methods were developed in the Thermal Science Lab at FIU for accurate filling process and were proven to be practical. Experimental testing has been performed and more than 20 watts of heat were transported by the heat pipe that has a vapor space of 82.5 by 4.1 by 1.27 mm <sup>3</sup> . In all cases, the temperature variation along the length of the substrate surface was less than 5 °C. The heat pipe was found to have an effective thermal conductivity greater than 10,000 W/m-K, which is over 300 times higher than that of the alumina it replaced within the substrate.					
15. SUBJECT TERMS Ceramic Heat Pipes, Electronic Cooling, Heat Pipe Fabrication, Liquid Charging, Heat Transfer					
16. SECURITY CLASSIFICATION OF:			17. LIMITATION OF ABSTRACT: SAR	18. NUMBER OF PAGES 52	19a. NAME OF RESPONSIBLE PERSON (Monitor) Brian Donovan 19b. TELEPHONE NUMBER (Include Area Code) (937) 255-5735
a. REPORT Unclassified	b. ABSTRACT Unclassified	c. THIS PAGE Unclassified			

# TABLE OF CONTENTS

<u>Section</u>	<u>Page</u>
List of Figures .....	iv
List of Tables .....	v
1. Introduction .....	1
2. Ceramic Heat Pipe Design .....	3
3. Fabrication Procedures .....	10
4. Liquid Charging .....	16
4.1 Micro-Syringe Method .....	20
4.2 Thermodynamic Equilibrium Method .....	23
4.3 Capillary Tubing Method .....	25
5. Heat Transfer Performance Test .....	27
5.1 HTCC Heat Pipes.....	27
5.2 LTCC Heat Spreader .....	34
6. Results and Discussion .....	36
7. References.....	37
Nomenclature.....	39
Greek Symbols.....	39
Subscripts.....	40
Acronyms .....	40

## LIST OF FIGURES

<u>Figure</u>	<u>Page</u>
1. Axial cross section of a typical heat pipe showing operating regions and fluid flows .....	2
2. Cross section of an axially grooved heat pipe wick, showing grooves on the top/bottom of heat pipe (left) and on the side walls of the heat pipe (right) .....	3
3. The effect on the capillary limit due to variations in groove width for groove depths of: (A) 0.64 mm, (B) 0.38 mm, and (C) 0.25 mm .....	7
4. The effect on the capillary limit due to variations in vapor space height for groove depths of: (A) 0.64 mm, (B) 0.38 mm, and (C) 0.25 mm .....	8
5. The effect on the capillary limit due to variations in vapor space height for groove widths of: (A) 0.10 mm, (B) 0.25 mm, and (C) 0.38 mm .....	9
6. Components of laser machined post-fired alumina heat pipe.....	12
7. Cross section of top-bottom grooved ceramic heat pipe.....	15
8. Cross section of sidewall-grooved ceramic heat pipe .....	15
9. Vacuum test setup .....	17
10. Vacuum test results.....	18
11. Micro-syringe filling setups.....	21
12. Filling setup for Thermodynamic equilibrium method .....	24
13. Thick-film heaters printed directly on one side of the heat pipe .....	29
14. Axial wall temperature distributions of CHP1 with heater 1 active.....	30

15. Axial wall temperature distributions of CHP1 with heaters 1 and 2 active.....	31
16. Axial wall temperature distribution of CHP1 with heaters 1,2,3 and 4 active .....	32
17. Axial wall temperature distributions of CHP2 with heater 1 active.....	34
18. Photograph of a LTCC heat spreader with an electronic component bound at the center of the top surface .....	35
19. Preliminary test results of LTCC heat spreader.....	36

## LIST OF TABLES

<u>Table</u>	<u>Page</u>
1. Primary results from thermodynamic equilibrium method.....	25
2. Test results of capillary tubing method (unit: mg).....	27

## 1. INTRODUCTION

The need to enhance thermal management at the packaging level of microelectronic components has become more critical. Many heat-related problems at this level constrain advances in microelectronics and optoelectronics technology today. The trend is that the power density will constantly increase. The projected power dissipation will exceed 200 watts per die by year 2005 [1]. Designers need more alternative means of thermal management at different levels to solve the problems. For high reliability under adverse environments, high and low temperature cofired ceramic substrates are typically used. However, the thermal conductivity of these materials is low, resulting in the need for enhanced thermal management technologies. Miniature heat pipes can be used to provide high thermal conductivity paths for this purpose. It has been demonstrated that miniature heat pipes can have effective thermal conductivities two to three orders of magnitude greater than that of typical substrate materials. Additionally, heat pipes have the characteristic of operating with a nearly uniform temperature across their length. Hence, fabricating miniature heat pipes as an integral part of a ceramic substrate can provide a thermal management solution for ceramic multichip module (MCM-C) packaging. A heat pipe consists of a sealed enclosure, with three distinct regions of operation: an evaporator, a condenser, and an adiabatic region separating the evaporator and condenser, as shown in Figure 1.

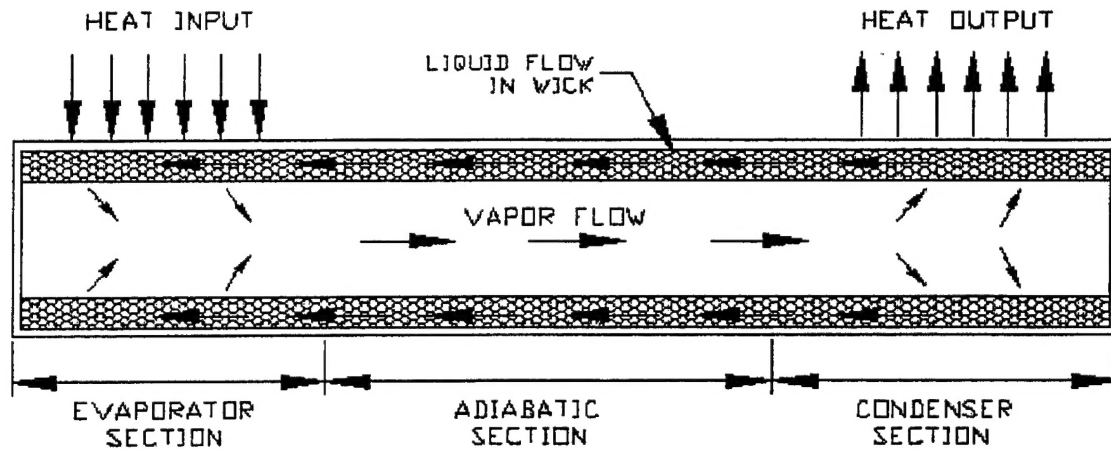


**Figure 1. Axial Cross Section of a Typical Heat Pipe Showing  
Operating Regions and Fluid Flows**

The heat pipe contains a working fluid, which absorbs heat by evaporation at the evaporator and travels as vapor through the adiabatic region to the condenser, where heat is removed, hence causing the vapor to condense back into liquid. The working fluid returns to the evaporator section through a wick structure by thermocapillary pumping action. The amount of heat energy (W or J/sec) that a heat pipe can transport relates to the heat of vaporization of the working fluid (J/gm) and the amount of material undergoing evaporation (gms/sec). The design of the wick is the most critical aspect to ensure high fluid transport, and thus high heat transport capability. The authors are focusing on two basic types of wicks compatible with cofire processing: the sintered (porous) wick and the axially grooved wick.



## 2. CERAMIC HEAT PIPE DESIGN

For use in MCM-C packaging applications, it will be desirable for the heat pipe to handle heat fluxes of up to  $40 \text{ W/cm}^2$  ( $250 \text{ W/in}^2$ ). Additionally, the geometry of the heat pipes will be on the scale of typical MCM-C packages. The most critical of the geometric dimensions is the thickness of the substrates, which is the smallest of the linear dimensions.

The most significant limiting factor in the power-handling capability of miniature heat pipes is the capillary limit, which is the point at which the wick cannot deliver working fluid at the same rate at which it is evaporated. This condition leads to evaporator dry-out, indicated by a rapid increase in the local temperature of the evaporator. The capillary limit is a function of the surface tension of the working fluid and the frictional forces caused by the interaction of the working fluid with the wick material and with the opposing vapor flow. The wick structures involved in this study are shown in Figure 2.

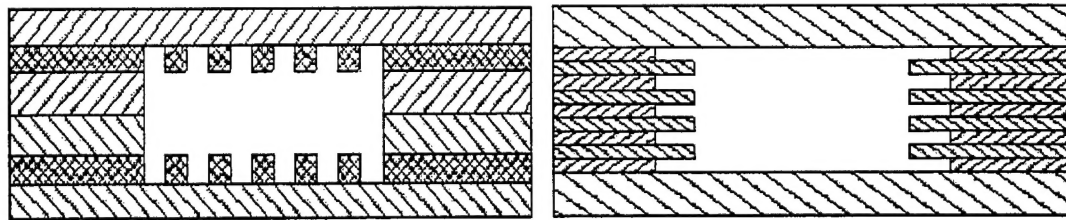


**Figure 2. Cross Section of an Axially Grooved Heat Pipe Wick,  
Showing Grooves on the Top/Bottom of Heat Pipe (Left)  
and on the Side Walls of the Heat Pipe (Right)**

The design of an optimized miniature heat pipe for the thermal management of electronics involves a complex balance of system requirements, and the thermophysics of heat pipes which involve capillary forces, phase change, two-phase flow interaction, and porous media and/or channel flow. The relevant issues will be discussed starting from the evaporator end of the heat pipe where the heat is generated, and will conclude at the condenser end where heat is removed.

At the evaporator end of the heat pipe, it will be desirable for the heat pipe to handle heat fluxes of up to  $40 \text{ W/cm}^2$  ( $250 \text{ W/in}^2$ ). This is roughly equal to the capability of removing heat from a single device dissipating 40 watts or removing 100 watts over its length from several devices.

The capillary limit is a function of the surface tension of the working fluid and the frictional forces caused by the interaction of the working fluid with the wick material and with the opposing vapor flow. For axially grooved heat pipes, the capillary limitation is given in Equation (1) [2], which relates the pumping action of the working fluid due to surface tension,  $\sigma$ , and the frictional forces,  $F_l$  and  $F_v$ , to flow of the working fluid from the condenser back to the evaporator. The frictional forces are described by two components:  $F_l$ , which represents the interaction of the working fluid and the wick material (structure), and  $F_v$ , which represents the resistance to the vapor flow due to the geometry of the vapor space.

$$Q_{CAP} = \frac{2\sigma}{w_g L_{eff} (F_l + F_v)} \quad (1)$$

The liquid and vapor frictional coefficients are given in Equations (2) and (3). Referring to Equation (2), it is seen that the permeability of the wick,  $K_g$ , is inversely proportional to the liquid frictional coefficient. Referring to Equation (3), it is seen that the vapor frictional coefficient is proportional to the friction factor,  $f(Re_{vh})$ , which is given by equation (5) [3].

$$F_l = \frac{\mu_v}{\rho_l A_w K_g h_{fg}} \quad (2)$$

$$F_v = \frac{\mu_v f(Re_{vh})}{2\pi R_{vh}^4 \rho_v h_{fg}} \quad (3)$$

The permeability of the axially grooved wick is given by Equation (4), which shows a ratio between the flow area and the friction to the flow. The friction factor,  $f(Re_{lh})$ , is determined using Equations (6) and (7), which include the shear stress interaction between the vapor flow and the liquid [4].

$$K_g = \frac{D_{lh}^2 \phi}{2f(Re_{lh})} \quad (4)$$

$$Re_{vh} = 24(1 - 1.355\alpha + 1.947\alpha^2 - 1.701\alpha^3 + 0.956\alpha^4 - 0.254\alpha^5) \quad (5)$$

$$\text{Re}_{lh} = \text{Re}_{lh0} \left\{ 1 + N_g \frac{w_g^3}{6\pi D_{vh}^3} \text{Re}_{vh} \frac{\nu_v}{\nu_l} \left[ 1 - 1.971 \exp\left(\frac{-\pi D_g}{w_g}\right) \right] \right\} \quad (6)$$

$$\text{Re}_{lh0} = 8D_g^2 \left\{ \frac{w_g^2}{4} \left[ 1 + 2 \frac{D_g}{w_g} \right]^2 \left[ \frac{1}{3} - \frac{32 w_g}{\pi^5 D_g} \tanh\left(\pi \frac{D_g}{w_g}\right) \right] \right\}^{-1} \quad (7)$$

All of the equations thus far show the paradox of miniature heat pipe design, i.e., the heat transport capability is increased by increasing the flow rates of vapor and fluid. However, a larger flow rate through small geometries leads to higher frictional losses, which decrease the heat transport. Hence, the optimization of the design parameters must be performed to provide a desired heat pipe design [5].

Insight into an optimal design can be gained by showing the effect of the groove depth,  $D_g$ , and width,  $w_g$ , on the capillary limit, as shown in Figure 3. From the figure, it is clear that an optimal groove width exists which is approximately the same for various groove depths (all other parameters held constant), and as the groove depth increases, so does the capillary limit.

In an effort to minimize the thickness of the heat pipe, it is desirable to minimize the height of the vapor space. The effect of the vapor space height is shown in Figure 4, which shows that the capillary limit initially increases sharply with increasing vapor space height, and then becomes relatively constant. Again, the effect of the groove depth is seen and follows the same trend as discussed for Figure 3. Important conclusions drawn from the figure are

that the minimum vapor space height is related closely with the depth of the grooves, and that additional vapor space height will not have any significant effect.

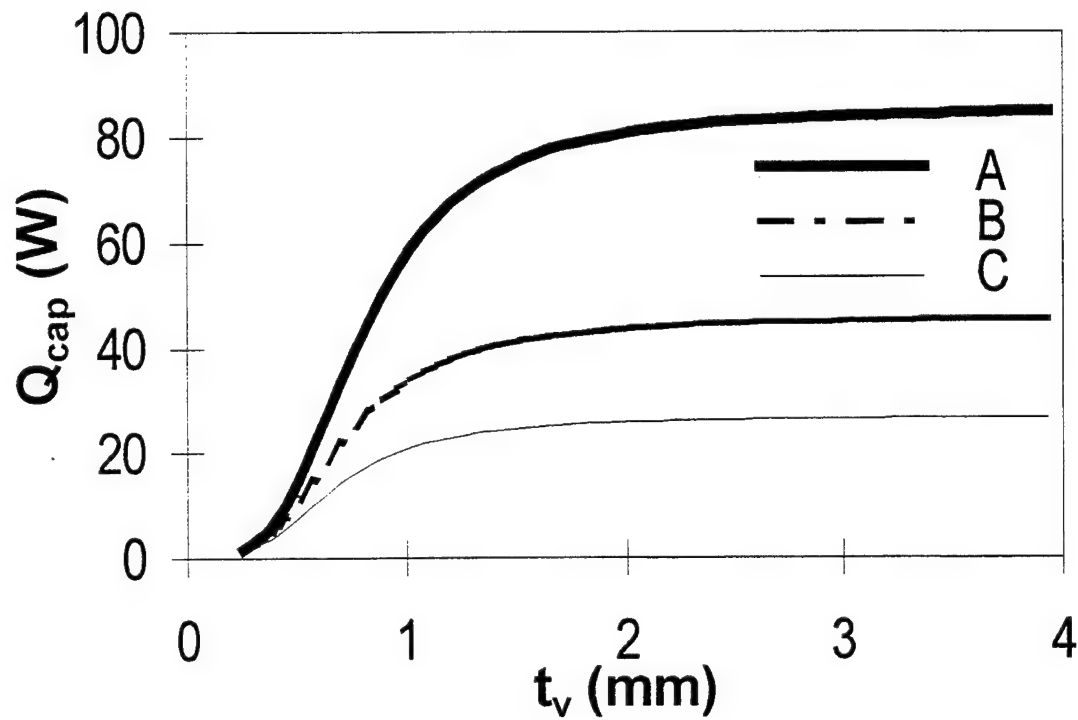
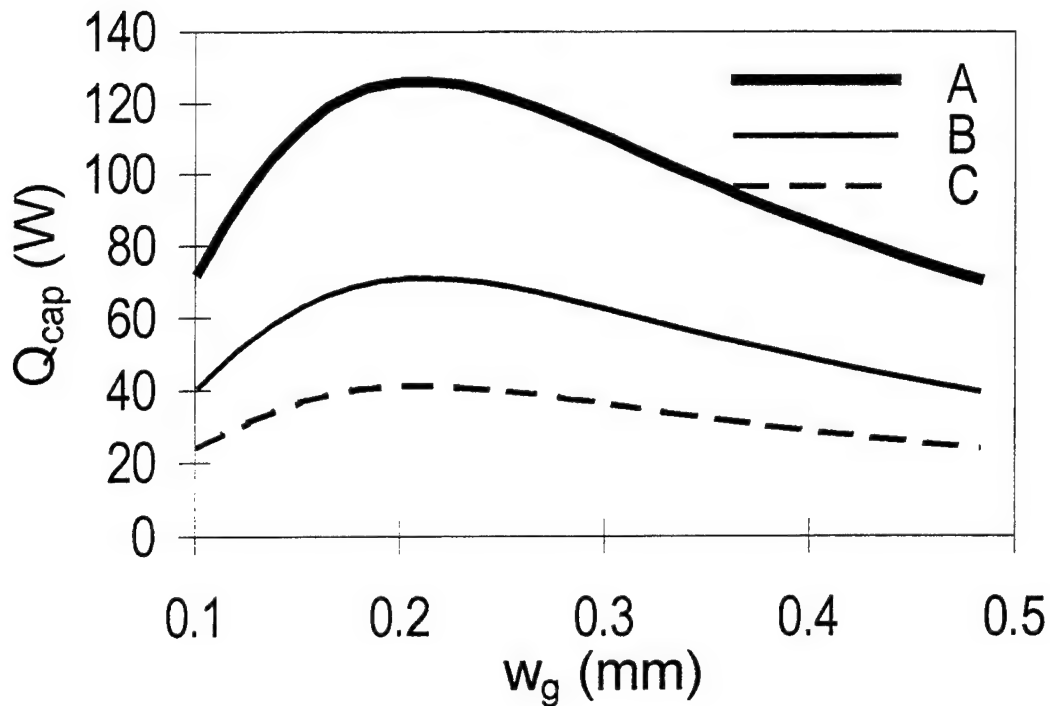


Figure 3. The Effect on the Capillary Limit Due to Variations in Groove Width  
for Groove Depths of (A) 0.64 mm, (B) 0.38 mm, and (C) 0.25 mm



**Figure 4. The Effect on the Capillary Limit Due to Variations in Vapor Space Height for Groove Depths of (A) 0.64 mm, (B) 0.38 mm, and (C) 0.25 mm**

The effect of the interaction between the groove width and the vapor space height is made clearer by holding the depth of the grooves constant and varying the other two parameters, as shown in Figure 5. The curves in the figure show that for small vapor space heights, smaller groove widths provide the highest capillary limit, but as the height of the vapor space increases, increases in the capillary limit are obtained with larger groove widths. The crossing-over effect shown by the curves indicates that there is a competition between

the shear stress interaction between the vapor and liquid flows and the ability of the wick to provide adequate mass of working fluid.

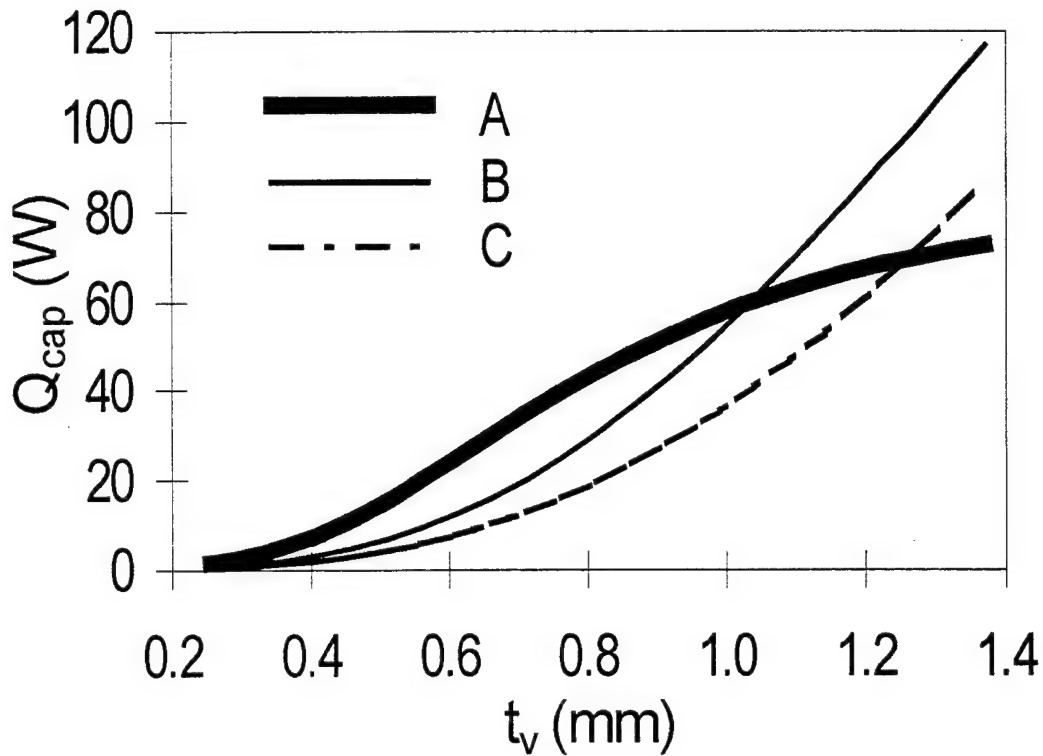


**Figure 5. The Effect on the Capillary Limit Due to Variations in Vapor Space Height for Groove Widths of (A) 0.10 mm, (B) 0.25 mm, and (C) 0.38 mm**

Small vapor space heights cause greater shear stress interaction; hence, only smaller groove widths can minimize the surface area of the working fluid interacting with the vapor flow. However, at some point, the vapor height is large enough that the shear stress

interaction becomes negligible and the capillary limit becomes strongly dependent on the cross-sectional area through which the working fluid can flow.

In concluding the discussion of the design issues for a miniature heat pipe, the conditions at the condenser end must be considered. As the goal is to cool electronics, the working temperature of the heat pipe needs to be between 25 and 110 °C. This range recognizes three thermal constraints:

- (1) Semiconductor junction temperatures must be below 150 °C; however, for reliability, derated temperatures typically are 110 and 125 °C.
- (2) Some additional thermal resistance will exist between the substrate and the semiconductor junction.
- (3) Typical coldplate and thermal contact areas have temperatures of 50 to 90 °C. Due to this thermal constraint, working fluids useful for the heat pipe would be water, ethanol-water, acetone, methanol, freon-22 and freon-11. For simplicity during this stage of the research, water was chosen as the working fluid.

### **3. FABRICATION PROCEDURES**

Two methods were used to form the wick structure and inner vapor space in this study: postfired laser cutting, and prior-laminated machining. At the very beginning, the former



was used to provide a rapid and relatively easy method of fabrication, allowing for various heat pipe designs to be built and tested for performance. In this manner, optimum designs can be determined and then fabricated in the latter technology.

The postfired heat pipe was fabricated using several pieces of  $\text{Al}_2\text{O}_3$  that were laser machined by Laserliance Technologies, Inc. All of the pieces had a length and width of 102 by 13 mm (4.0 by 0.50 in) with a thickness of 0.6 mm (0.025 in). Four types of patterns were used in the design to provide a top and bottom shell, axially grooved wicks, and spacers, as shown in Figure 6.

The layers of the heat pipe were bonded together using Heraeus SG-683K dielectric thick film paste, which was stenciled onto the alumina with an approximate thickness of 0.25 mm (10 mil). To allow for soldering of a metal filling tube to the ceramic, a silver-platinum metalization (Heraeus C4740S conductor thick film paste) was patterned around the fill hole in the top shell. The assembly was fired in two cycles, the first for the metalizations and the second for the glass. After firing, a 1.6-mm (0.0625 in.) outside diameter copper tube and flange assembly was soldered to the heat pipe.

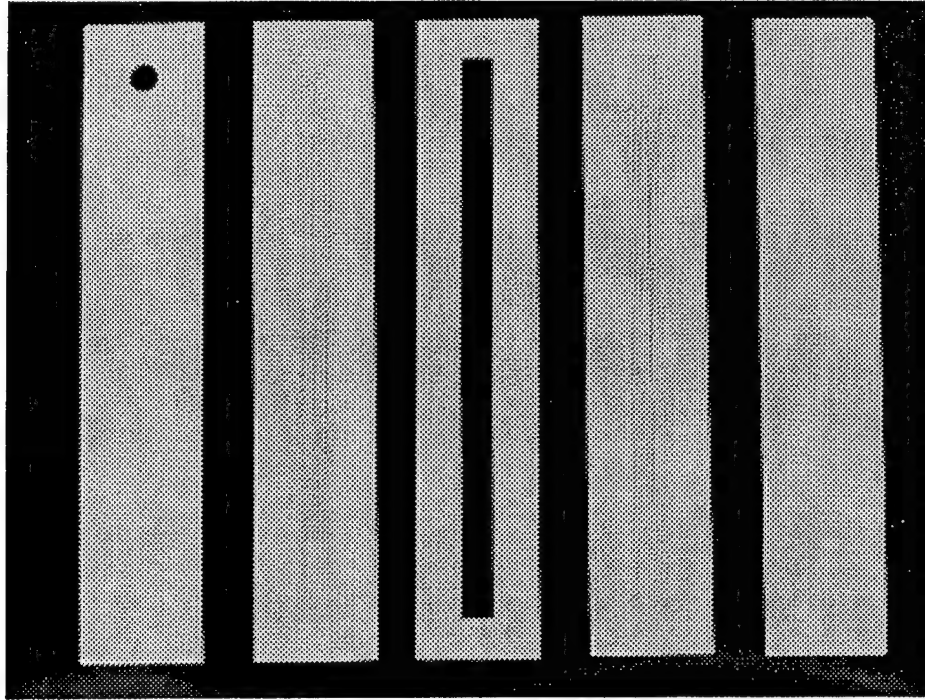


**Figure 6. Components of Laser Machined Postfired Alumina Heat Pipe**

The prior-laminated machining fabrication of a heat pipe within ceramic cofire materials requires an open channel to be built before cofiring. This leads to the primary concern of sagging of the green tape on the top and bottom layers of the substrate during the firing cycle. This would ultimately affect the flatness of the substrate. Hence, to minimize the potential for sagging or at least to keep the flatness of the substrate acceptable, the width of the heat pipe should be minimized, with the width of heat pipes being 1.3 to 7.6 mm (0.050 to 0.300 in). Furthermore, substrates by their nature are thin; hence, the thickness of the substrate dictates a heat pipe with a height on the order of 0.6 to 2.5 mm (0.025 to 0.100 in).

The fabrication of an efficient wick structure must be compatible with ceramic materials and conventional manufacturing processes. Wick materials would have to adhere to

ceramic materials, and not oxidize or burnoff during the high temperature firing cycle.

Axially grooved wicks would require the patterning of very thin, long, and closely spaced slots into the green tape with the resolution of typical electrical interconnections.

Additionally, these fine slots would have to remain intact during lamination and firing processes.

The fabrication of a miniature heat pipe in cofire ceramic requires that the structure of the heat pipe be compatible with the cofire ceramic structure, which is a lamination of several layers of ceramic tape to form a single monolithic structure. For low temperature cofire ceramic (LTCC), the process involves lamination pressures of 20.6 MPa (3000 psi), and a firing temperature of 850 °C, whereas, for high temperature cofire ceramic (HTCC), the firing temperature is elevated to over 1600 °C.

The vapor space for the heat pipe can be easily formed in the cofire tape stack by punching slots in each layer of tape. Stacking several layers of tape with the slots cut into them forms a long rectangular duct within the substrate. The fabrication of the axial grooves for the wick structure involves two groove sets: top/bottom and sidewall.

Axial grooves in the top and bottom interior surfaces of the heat pipe have to be fabricated by numerically machining small grooves into the top and bottom tape layers of the heat pipe's outer shell. The process requires the use of micro endmills and a numerically controlled, three-axis machining system with a precision of at least 0.025 mm. In contrast, the fabrication of axial grooves in the sidewalls of the heat pipe are relatively easy. These grooves are formed by varying the width of the rectangular slot cut into each tape layer to form the vapor space. The variation in the widths of the slots on alternating layers provides control over the depth of the grooves. However, the width of each groove is

dictated by the thickness of the tape layers. Fortunately, typical cofire tape is 0.10 to 0.25 mm thick, which allows fine narrow grooves to be formed.

The cross sections of the cofired heat pipes are shown in Figure 7 and Figure 8. The dimensions were obtained from the measurement of photomicrograph and are slightly different from the designed sizes due to the deforming and shrinking in the lamination and cofire process, as well as the machining errors. Obviously, there are also some measurement uncertainties involved. Although the sidewall-grooved wick structure looks irregular in shape, it works well as capillary wick.

A new approach, which is totally different from the conventional mechanical cutting method, is being developed to form wick structure and vapor space. An organic insert that contains the desired structure is inserted into the rectangular slot during lamination, and the ceramic undergoes viscoelastic flow to conform to the surface of the insert. During firing, the insert volatilizes and is removed. This allows a uniform green density to be achieved during lamination, minimizing sag and other problems. However, this technique was not developed during this work, but is discussed to indicate that a solution to the development of a complex wick structure has been achieved.

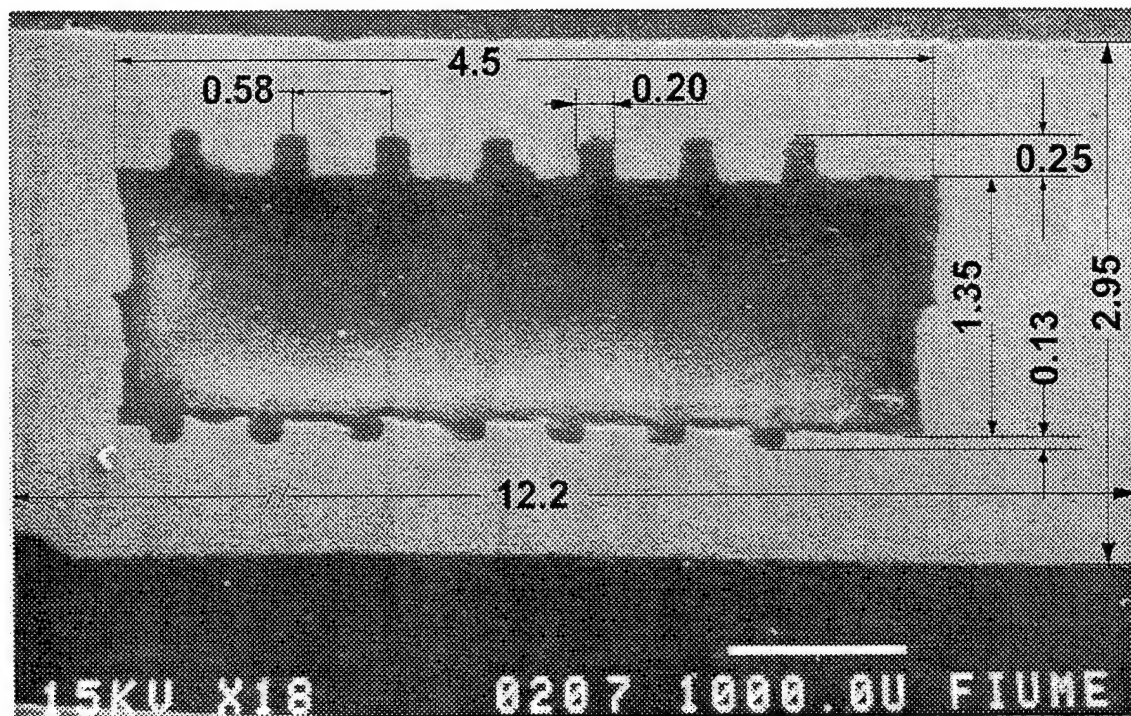


Figure 7. Cross Section of Top Bottom Grooved Ceramic Heat Pipe

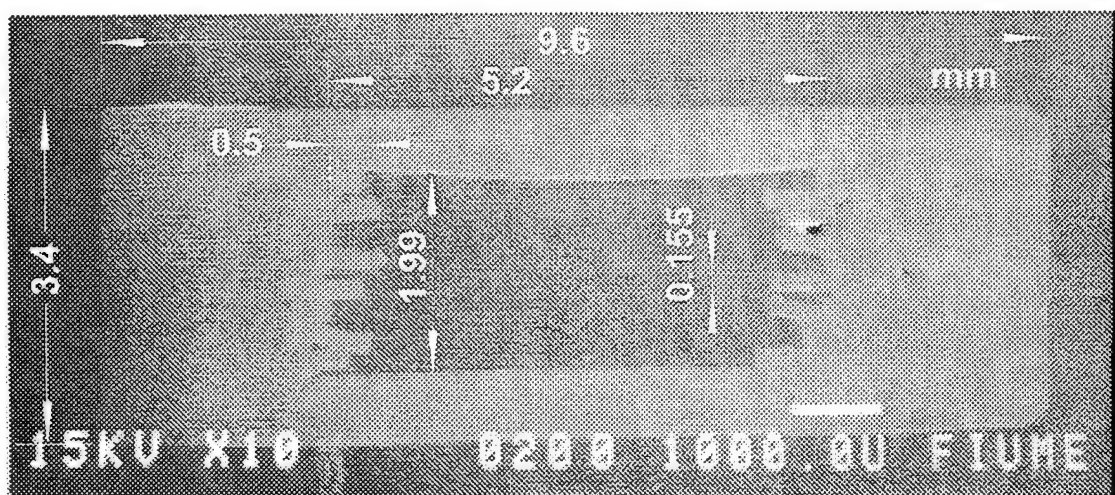


Figure 8. Cross Section of Sidewall-Grooved Ceramic Heat Pipe

#### 4. LIQUID CHARGING METHODS

Liquid charging is critical to any micro/miniature heat pipes [6,7]. It is extremely difficult to precisely measure and control a small amount of working liquid on the order of 0.01 grams in a vacuum environment. The performance of a micro/miniature heat pipe, however, is very sensitive to the quantity of working liquid charged. A small variation in the charge can degrade the heat pipe performance and even make the heat pipe not function at all.

The effects associated with less liquid include premature dry-out at the evaporation section due to an unsaturated wick structure. The dry-out causes a rapid increase in the local temperature; hence the electronic components being cooled by the heat pipe can suffer thermal failure. A large temperature gradient at the evaporator section experiencing dry-out can also cause a failure in the ceramic material due to thermal stress and/or thermal shock. Overcharging the heat pipe can lead to a flooded and blocked condensation section by the excess liquid. This challenge is further complicated by the necessity of an initial high vacuum and its maintenance during the liquid charging process.

An initial high vacuum itself is difficult to obtain in micro/miniature heat pipes via a small diameter filling tube. A simple test was conducted to simulate this environment. The setup, as shown in Figure 9, consists of a turbo molecular vacuum pump system and two vacuum meters located at both ends of a Tygon manifold. The sensor of vacuum meter 1 is mounted directly at the pump inlet port and that of vacuum meter 2 is connected via a

small tube at the other end. The two sensors are 1 meter apart. The small tube represents the typical filling tube of a miniature heat pipe. The small tube has a length of 40 mm and an inside diameter of 0.88 mm.

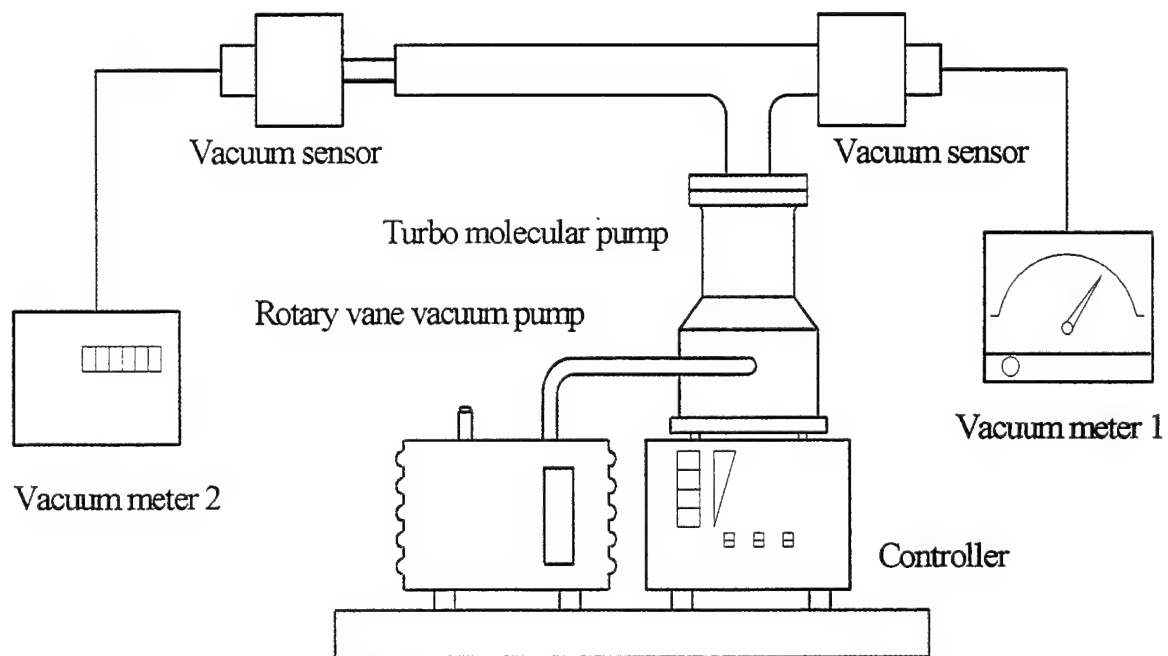


**Figure 9. Vacuum Test Setup**

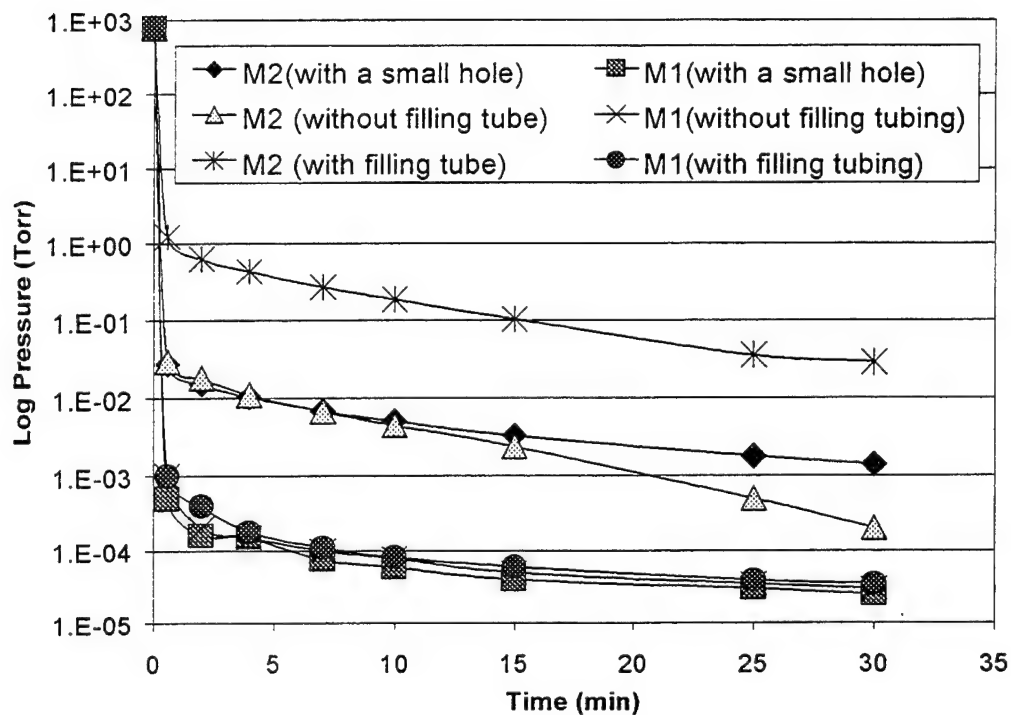


**Figure 10. Vacuum Test Results**

For comparison, the test was carried out with or without the small tube or with just a 1.6 mm of hole. The results are shown in Figure 10. It can be seen from the figure that an obvious vacuum difference exists between the two meters. With a small filling tube, it is difficult to develop high vacuum inside the heat pipe. After evacuating for 30 minutes, the pressure reading of meter 2 is still above  $10^{-2}$  Torrs. The knowledge of this situation is important choosing the liquid charging methods.



Plesch et al. [8] charged their miniature copper heat pipes with dimensions of 7 by 2 by 120 mm<sup>3</sup> by introducing condensing water vapor. They indicated that it was not possible to control and determine the amounts of water present during the process of filling. After pinching off the fill tubes, the amount of charge was determined by weighing the charged heat pipe. More than 0.15 grams of liquid was required, which is much more than that in the current study. They mentioned that a filling station was under construction which would allow very small amounts of degassed clean water to be metered in. But the followup report has not been seen.

Badran et al. [9] tested a micro heat pipe array anisotropically etched on a single crystalline semiconductor silicon wafer. Two sets were fabricated, each of which had 73 and 127 micro heat pipes, respectively, in the silicon wafer. The condenser section of the heat pipe array was connected to a common reservoir for filling procedures. In order to measure the amount of working liquid visually, a Pyrex glass wafer was used to seal the pipe array. Similarly, Duncan and Peterson [10] charged their micro heat pipe array visually one by one. The heat pipes were sealed also by a 200- $\mu$ m-thick Pyrex glass and were evacuated to a pressure of  $10^{-3}$  Torrs. A working liquid was introduced with the aid of a syringe and a trough. The vapor became trapped in the evaporator end and the fluid filled the remaining volume of the heat pipes. The wafer was removed from the vacuum system while being heated from the evaporator end. The extra liquid was then removed by vapor expansion until the desired fluid quantity was measured via a caliper visually through Pyrex glass. This method is similar to the boiling degassing method for conventional heat pipes, which is unreliable for micro/miniature heat pipes due to the very small charge volume.

Benson et al. [11] tried to measure the methanol quantity during the filling process by pumping the fully filled heat pipe through a series combination of a needle valve and heated capillary tubing. The tubing was heated up to 125 °C, ensuring that the fluid passing through was in the vapor state to allow metering. The heat pipe array was immersed in a temperature-controlled bath maintained at 26 °C during the vacuum pumping process. By monitoring the pressure change, the full evacuating time needed for the heat pipe array to reach the completely dry state was determined previously. Then by pumping out the fully filled heat pipe array for a fraction of the full time, for example, 80 percent, the remaining liquid would be 20 percent of the initial volume. This is correct under the assumption that a linear relationship exists between mass removal rate and the pumping time.

To sum up, there is no existing charging method available for our ceramic heat pipes. It is necessary to develop a reliable and practically feasible charging method. Three methods have been developed for charging micro/miniature heat pipes. Within the following discussion, these methods will be referred to as the microsyringe method, the thermodynamic equilibrium method, and the capillary-tubing method.

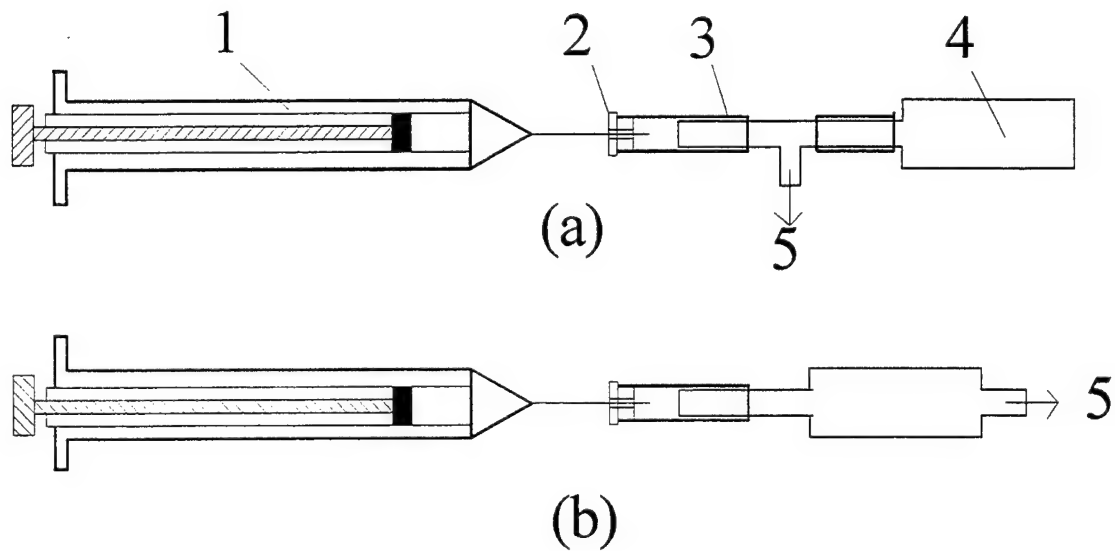
#### **4.1 Microsyringe Method**

A unique micro-syringe, designed primarily for precision measurement and displacement of liquid or gaseous samples into chromatographic analyzers, was used in this method. The syringe consists of a turn valve with a Teflon seal, a leak-tight Teflon plunger tip, and a removable needle. This type of syringe is recommended for use in either a high vacuum or with pressures up to 250 psi, with gases or liquids. The turn valve can be used to isolate

the working fluid stored in the barrel from the vacuum during evacuating of the heat pipe.

The plunger makes flush contact with the bottom of the syringe barrel when fully depressed, virtually eliminating any dead volume.

The filling setup is schematically shown in Figure 11.



1-Microsyringe; 2-Teflon seal; 3-Polyurethane tubing;

4-Heat pipe; 5-To vacuum system.

**Figure 11. Micro-syringe filling setups**

The heat pipe is connected to the syringe using the polyurethane/Teflon adapter through which the needle is inserted. There are two methods to make the connection of the heat

pipe with the vacuum system. One is completed through a T-junction, as shown in Figure 11(a). The other is similar in nature, except for the elimination of the T-junction and the addition of an evacuating tube on the other end of the heat pipe that is used for evacuating air out of the heat pipe. The filling procedure for the system incorporating the micro-syringe and the T-junction can be outlined as follows:

- (1). Fill the syringe with the working liquid.
- (2). Lock in the liquid. Replace the needle with a dry one and lock in the working liquid in the barrel by screwing the nosepiece with at least two turns left to be tightened. At this time, there is no liquid in the needle, and the liquid is isolated from the ambient.
- (3). Evacuate the heat pipe. Connect the syringe with the heat pipe through the T-junction and connect the T-junction to the vacuum system, until the desired vacuum is reached. The vacuum inside the heat pipe is difficult to measure and is certainly lower than the system vacuum because of the small diameter of the filling pipe. Adequate time should be allowed for the heat pipe to reach the desired vacuum.
- (4). Fill the heat pipe. Screw the needle nosepiece all the way and depress the plunger down to the dead point to displace the working liquid into the heat pipe via the filling tube.
- (5). Finally, pinch and seal the heat pipe filling tube.

The procedure for the second method is similar to that for the first one except that the vacuum system is connected to heat pipe through the evacuating tube. After evacuating the heat pipe, but prior to charging, the evacuating tube must be sealed by crimping. Then, the charge can be injected into the heat pipe.

To prevent the liquid from flashing back into the connection tube during the injection, a tiny inner Teflon seal was mounted as close to the end of filling tube as possible. The inner

seal is very important to control the correct quantity of liquid. The inside diameter of the inner seal is 0.7 mm. The presence of the inner seal further increases the difficulty in establishing high vacuum in the heat pipe.

#### **4.2 Thermodynamic Equilibrium Method**

The thermodynamic equilibrium method, as its name indicates, is based on the thermodynamic equilibrium principle. The system, shown in Figure 12, is composed of three parts – a steam generator, a vacuum pump system and a vacuum chamber. The steam generator is actually a two-phase closed thermosyphon, which generates pure liquid and maintains a pressure needed to push liquid into the heat pipe. After the interior of the heat pipe is evacuated to a desired vacuum, the condensate from the condenser is introduced into the heat pipe through the filling tube to completely fill the interior volume. The pressure in the heat pipe at this time is the same as that of the evaporator, which can be adjusted by changing the working temperature. At this point, the valve V2 is closed to isolate the two vacuum volumes from the steam generator. Valve V1 is now opened, exposing the charge in the heat pipe to a high vacuum, resulting in vapor flash of the charge liquid. Consequently, the pressure in the vacuum chamber increases and a thermodynamic equilibrium point is eventually achieved. The amount of liquid flashed out is mainly determined by the volume of the chamber. On the other hand, the wick structure inside the heat pipe would attempt to hold liquid to the extent that the structure gets saturated. The thermodynamic equilibrium method seems to meet the requirements automatically. However, this method needs careful calibration for each heat pipe volume to be changed. During the process of flashing, the temperature of the heat pipe decreases

because of the endothermic evaporation process, suppressing the flashing process unless the heat pipe is immersed in a constant temperature bath. Sealing the heat pipe before the equilibrium is reached would overcharge the heat pipe. Table 1 lists some test results from the thermodynamic equilibrium method. Tests were conducted by weighing the heat pipe before and after charging while it was temporarily sealed. It can be seen from the table that the error seems to be acceptable. The disadvantages are the unpredictability of liquid charging quantity and unease in the control of the factors that affect the charging process.

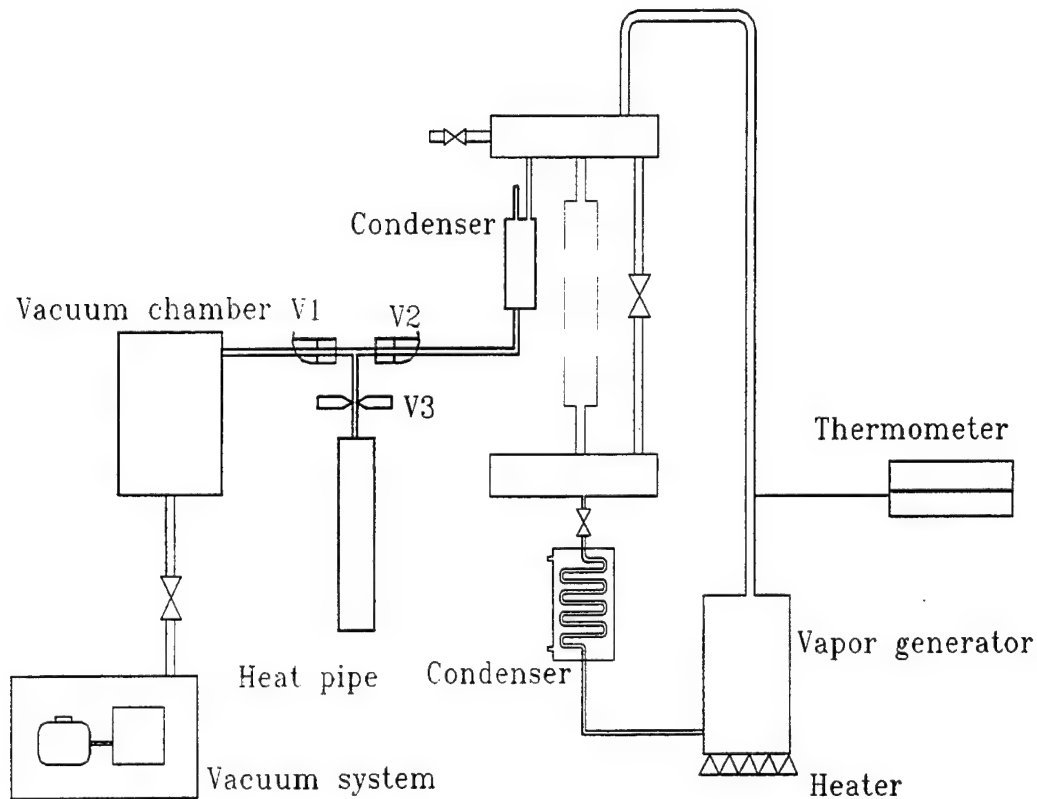


**Figure 12. Filling Setup for Thermodynamic Equilibrium Method**

**Table 1. Primary Results from Thermodynamic Equilibrium Method**

Chambers	Volume (ml)	Liquid charges (g)	Average (g)	Deviation range
1	1890	0.085, 0.117, 0.097, 0.080, 0.102	0.0962	-0.0162~0.0208
2	500	0.149, 0.132, 0.144, 0.152, 0.165	0.1484	-0.0164~0.0166

#### **4.3 Capillary Tubing Method**

Evolved from the thermodynamic equilibrium method, the capillary tubing method uses a capillary tubing instead of the vacuum chamber of the thermodynamic equilibrium method. The idea is based on the following facts. The volume of working liquid is a fraction of the whole interior volume. For the ceramic heat pipes studied in this report, the total volume is 0.512 cc and the working liquid needed is about 0.07 cc, which is less than 14 percent of the total volume. Controlling the filling amount of 0.07 cc is difficult, but measuring the rest of the volume is much easier. The capillary tubing method uses a long tubing with a small inside diameter to remove the liquid from the completely filled heat pipe. The removed quantity of liquid depends on the length and diameter of the capillary tubing. The measurement of the volume of the working liquid was converted into the measurement of the tubing length. The charging procedure is similar to the thermodynamic equilibrium method, as outlined as follows:

- (1). Fill the heat pipe completely using condensate from the condenser after evacuating.
- (2). Connect the capillary tubing to the fully filled heat pipe.
- (3). Evacuate the capillary tubing.
- (4). Isolate the capillary tubing from the vacuum system.
- (5). Heat the heat pipe up to above 60 °C, forcing the liquid into the capillary tubing and eliminating the possible vapor bubbles in the liquid by using the elevated pressure.
- (6). Seal the heat pipe when the capillary tubing is full of liquid.

By contrast to the thermodynamic equilibrium method, the liquid removal is implemented by pushing the extra liquid into the capillary tubing, but not by flashing. The liquid quantity is controlled by the volume of the capillary tubing. Every factor in this method is controllable.

Some results obtained from this method are shown in Table 2. Like the test of thermodynamic equilibrium, the remaining liquid in the heat pipes is determined by weighing. A transparent Tygon tubing with an inside diameter of 1.5 mm is used as the capillary tubing in order to achieve visualization. Two heat pipes, HP1 and HP2, were tested. The former was a copper miniature heat pipe and the latter was a ceramic one with 0.79 cc and 0.72 cc of vapor space respectively.

In summary, the syringe method is the easiest to accomplish in a lab and is the most accurate. Its disadvantage is that the initial vacuum directly affects the performance of the heat pipe. Also, the liquid preparation process is exposed to air, and it is not suitable for mass production. The thermodynamic equilibrium method is feasible, but it has several disadvantages. Accurate calibration can be made only by trial and error. The capillary tubing method is recommended because of its reliability and accuracy.



**Table 2. Test Results of Capillary Tubing Method (unit: mg)**

HP1	Prediction	88	176	352	440	528	
	Test value	89	181	361	450	534	536
	Difference	1	5	9	10	6	8
HP2	Prediction	60	95	191	381	477	572
	Test value	64	101	187	382	482	574
	Difference	4	6	-4	8	6	22

## **5. HEAT TRANSFER PERFORMANCE TEST**

### **5.1 HTCC Heat Pipes**

Preliminary testing has been performed on two HTCC heat pipes with grooves on the top and bottom or on the sidewalls. For simplicity in the following discussion, the tested heat pipes will be referred to as CHP1 and CHP2, respectively. The results of the testing will be discussed here as an example of the typical performance characteristics to be expected by embedded heat pipe in MCM-C substrates. Of particular importance is the temperature variation from the evaporator to the condenser and the maximum amount of heat that could be dissipated at the condenser before the wick began to dry out.

To provide a heat source, four thick-film heaters were printed directly on one side of the heat pipe along the axial direction uniformly for different heating models, as illustrated in

Figure 13. A variable transformer was used to adjust the heater's heat load, which was determined by measuring input voltage and current. Seven thermocouples were placed on the heating section. To reduce heat losses to the ambient, the evaporation and adiabatic section of the heat pipe were insulated from ambient conditions using fiberglass tape. The amount of heat loss was taken into account by calculating the natural convection based on the surface temperature of the insulation. Cooling was accomplished by clamping a finned copper heatsink on the condensation section with silicon grease on the interfaces for contact resistance reduction. The contacting area was about  $1.7 \text{ cm}^2$ . The finned heatsink was cooled by natural convection or forced convection through a small fan similar to those used in the computer cooling. It is worth noting that the heating method in the present study is different from that using Kapton foil heater in most of the previous studies [12]. When the foil-heater heating is used, the axial temperature distribution might be much flatter, because of its indirect heating and the temperature measurement not from underneath the heater. By contrast, in the present study, the temperatures were taken on the centerline between heaters in the evaporation section. They would be much closer to the heaters' temperature.

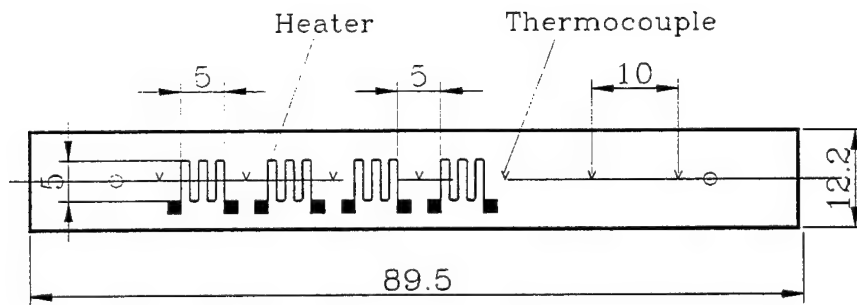


**Figure 13. Thick-Film Heaters Printed Directly on One Side of the Heat Pipe**

The axial temperature distributions for CHP1 are shown in Figure 14 through Figure 16 with 1-, 2- and 4-heater bottom heating modes, respectively, when the heat pipe was running horizontally. Figure 14 shows the same characteristics for CHP2 with only heater 1 active.

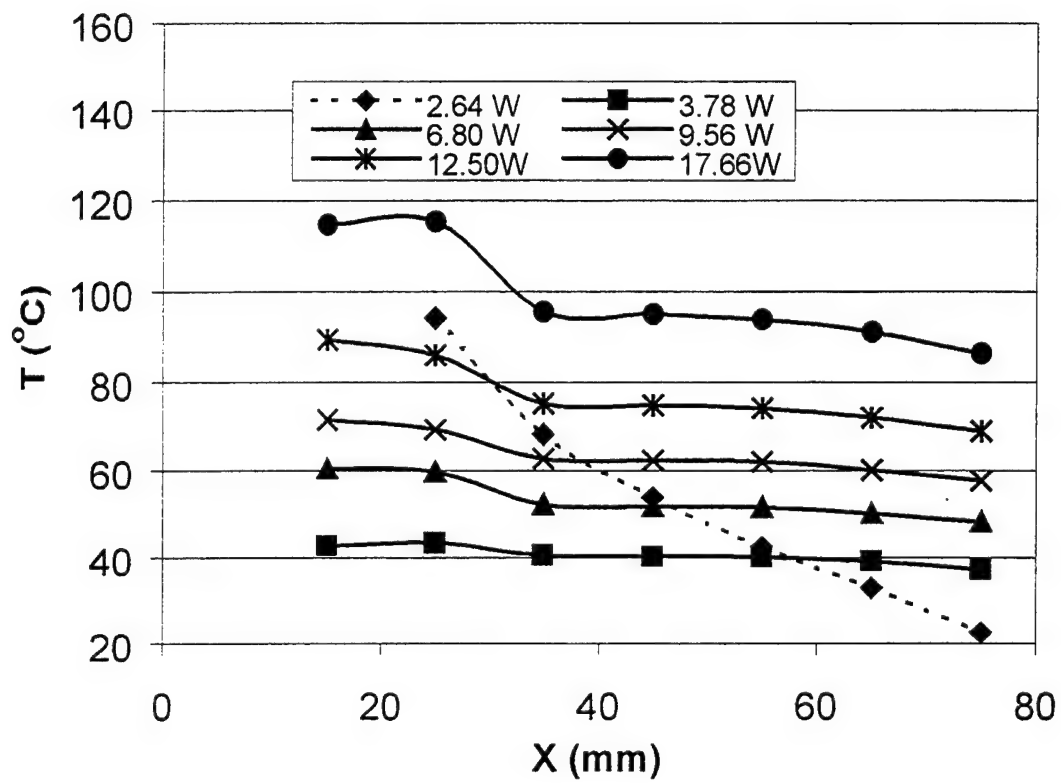


Figure 14. Axial Wall Temperature Distributions of CHP1 with Heater 1 Active

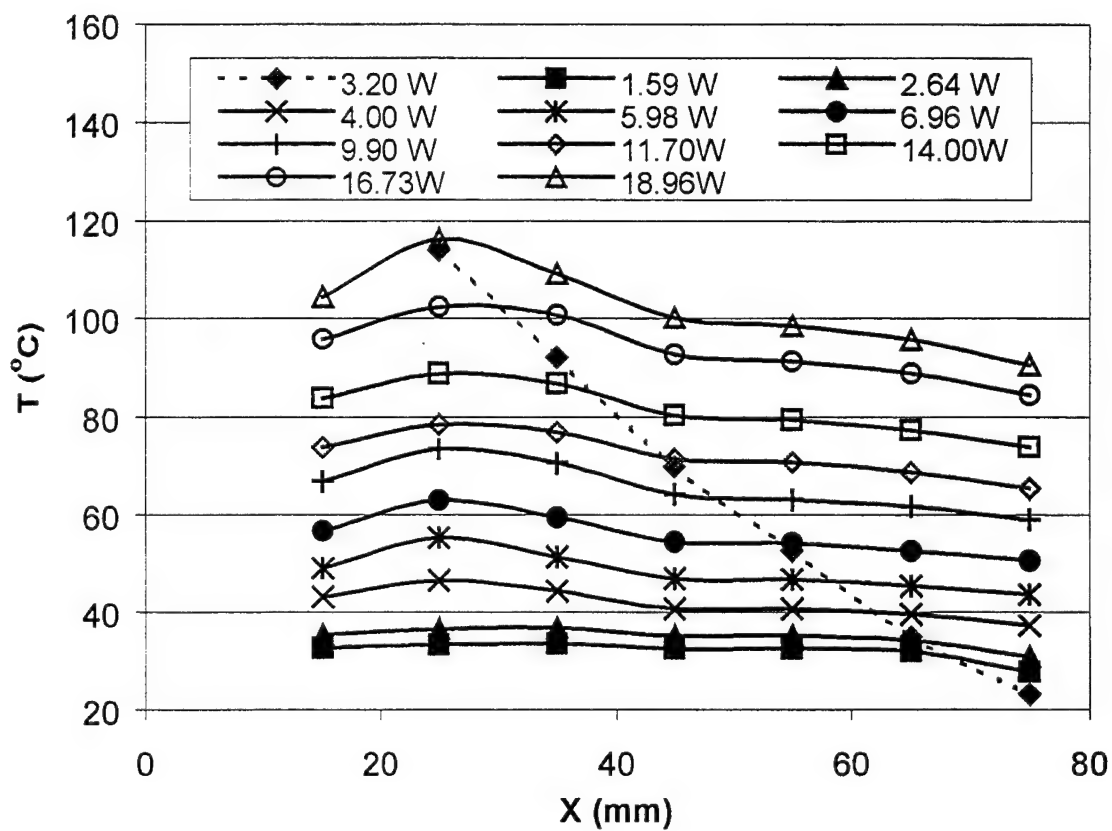
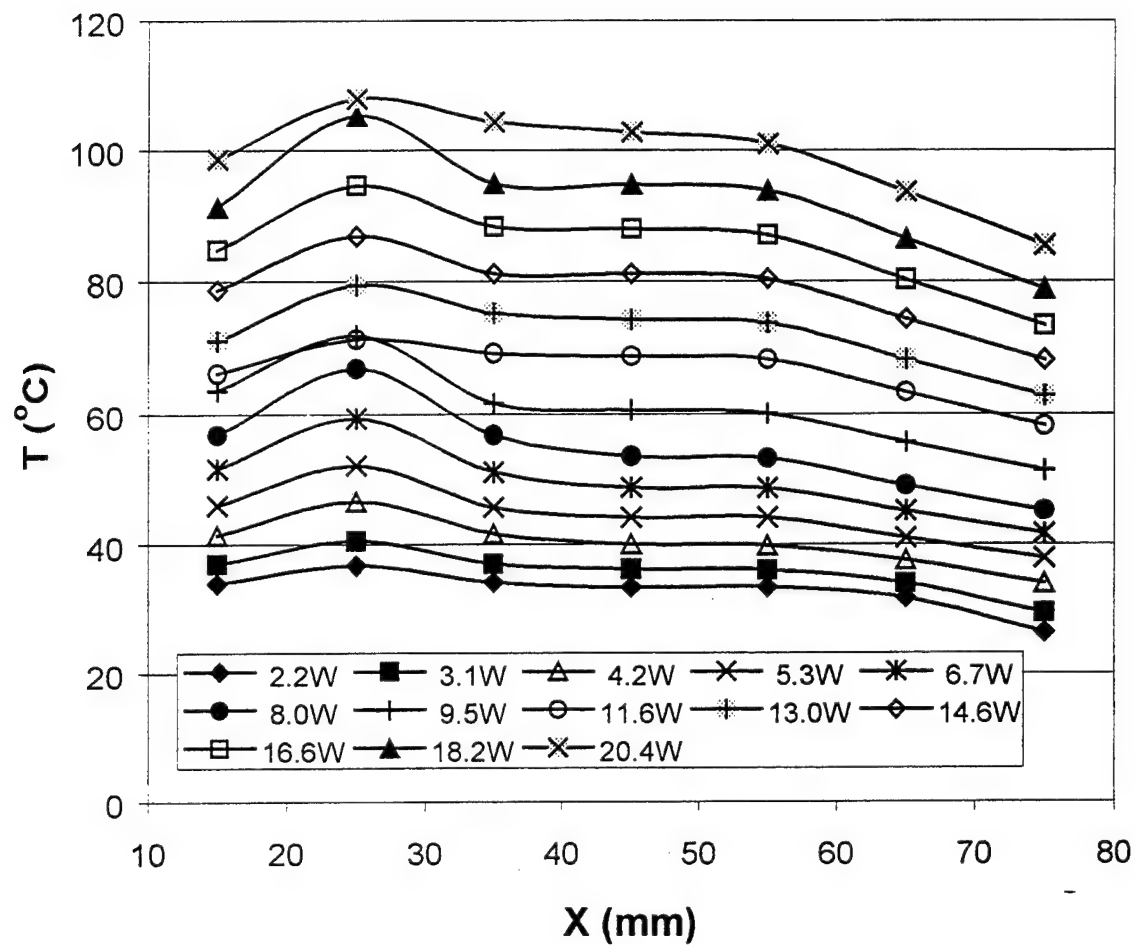
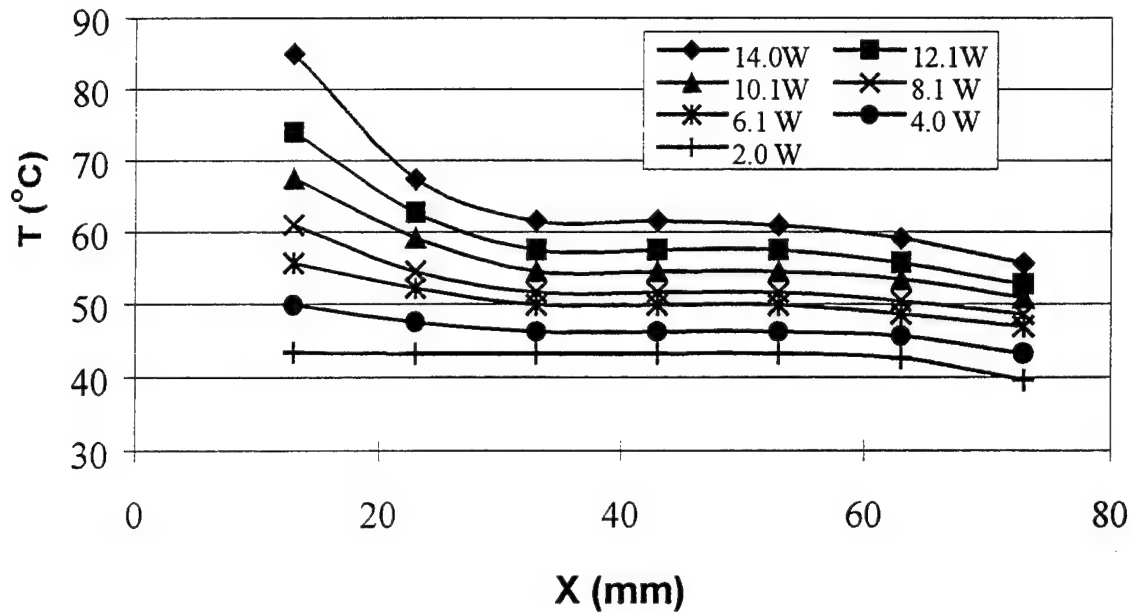


Figure 15. Axial Wall Temperature Distributions of CHP1  
With Heaters 1 And 2 Active



**Figure 16. Axial Wall Temperature Distribution of CHP1  
with Heaters 1, 2, 3 And 4 Active**

For visual comparison, the dotted and dashed lines in Figures 14 and 15 represent the temperature distributions of a solid ceramic bar with the same overall dimensions and the same heating mode. The CHP2 has a different profile in the evaporation section with a hot spot at the end, especially at high heat flux, as shown in Figure 16. This is possibly caused by a local dry-out resulting from the nonwick evaporating surface. The coarseness of the ceramic surface is not adequate to provide enough liquid for high powers. The heat must be conducted to the grooved sidewall through a longer distance with a higher conduction temperature difference. It is worth noting that the maximum heat transfer of the heat pipe was not reached in this experiment. The line heat-source heating method may cause the ceramic shell to crack at a high temperature gradient. Therefore, of particular interest are the temperature differences between the evaporation section and adiabatic section, which includes the conductive temperature difference across the shell and groove-liquid film and the evaporation temperature difference at the liquid-vapor interface if the thermal resistance due to vapor flow between evaporation and adiabatic section can be ignored. They increase with the heat input and are much bigger than those in metal heat pipes as shown in Figure 17. It can be seen from the figure that the temperature difference is relatively high, especially at a high heat flux. It reaches 20 °C at 18.72 W of heating power, corresponding to 75 W/cm<sup>2</sup> of heat flux for CHP1. The CHP2 has a similar trend to CHP1. It would be much higher for the LTCC because of the lower thermal conductivity. Consequently, a thermal-via technology is being developed for the evaporation and/or condensation section to increase the conductivity of the shell and reduce the temperature difference. In general, the temperature difference due to the condensation heat transfer in



**Figure 17. Axial Wall Temperature Distributions of CHP2 with Heater 1 Active**

this situation is less important because the heat dissipation area in this section can be much larger than the heating area, which results in a much lower heat flux.

## 5.2 LTCC Heat Spreader

An LTCC-water heat spreader was fabricated and tested at Harris Corporation. An electronic component was directly bound at the center of the top surface of the heat spreader, as the photograph in Figure 18 shows. A specially designed power supply and control unit was used to make the component function as in practice. The spreader's



bottom surface was pressed down onto a constant-temperature cold plate. A thermocouple was mounted on the top surface of the component to monitor the temperature. Figure 19 illustrates the preliminary test results with and without the heat spreader and indicates that the heat spreading effectiveness is very obvious. It is promising to have several fold increase in power for this kind of electronic component.

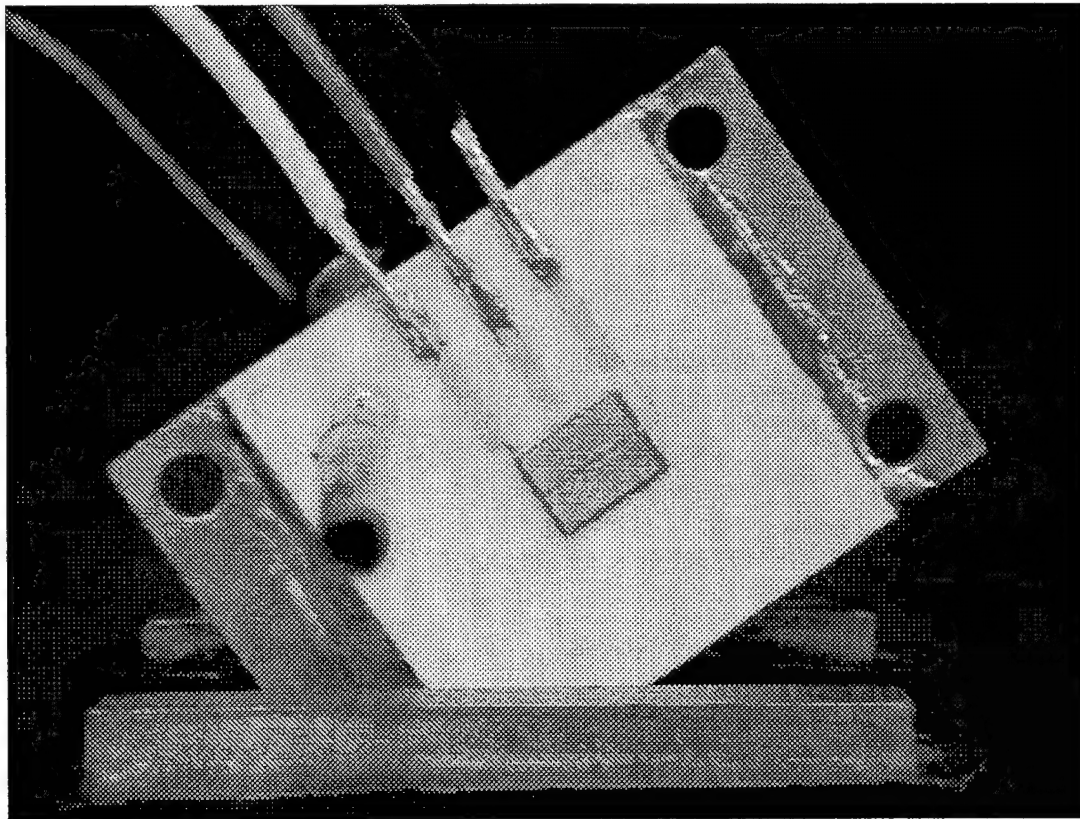


**Figure 18. Photograph of A LTCC Heat Spreader  
with an Electronic Component Bound at the Center of the Top Surface**

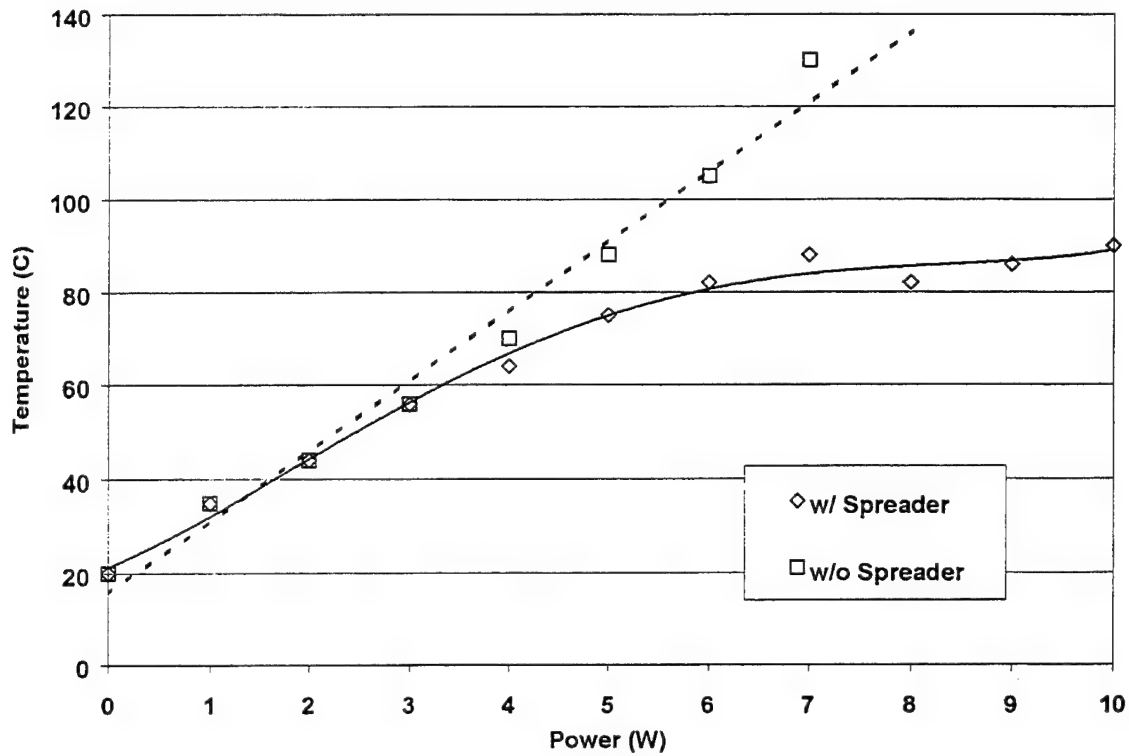


Figure 19. Preliminary test results of LTCC heat spreader.

## 6. RESULTS AND DISCUSSION

In this study, the fabrication process of HTCC and LTCC was explored and the miniature heat pipes were successfully integrated into substrate made of HTCC and LTCC, while a brand new wick-forming approach is being developed. Three types of liquid filling method were developed and successfully used in the filling process, among which the capillary tubing method is recommended by the authors. The heat transfer performance of the

HTCC/LTCC heat pipes was tested and satisfactory results were obtained. More than 20 watts of heat were transported by the HTCC heat pipe that has a vapor space of 82.5 by 4.1 by 1.27 mm<sup>3</sup> with cooling provided along the condenser region by natural convection or by a temperature-controlled cooling jacket. The temperature variation along the length of the substrate surface was less than 5 °C. The HTCC heat pipe was found to have an effective thermal conductivity greater than 10,000 W/m-K, which is over 300 times higher than that of the alumina it replaced within the substrate. An LTCC heat spreader was used to cool an electronic component from Harris Corp. The preliminary test indicates that the working temperature was greatly decreased at high power output.

## 7. REFERENCES

1. Semiconductor Industry Association, "Technology Roadmap," 1995.
2. Faghri, A., Heat Pipe Science and Technology, Taylor and Francis, Washington, D. C., 1995.
3. Shah, R.K., and Bhatti, M.S., "Laminar Convective Heat Transfer in Ducts", in Handbook of Single-Phase Convective Heat Transfer, Eds., Kakac, S., Shah, R.K., and Aung W., Wiley, New York, 1987.
4. Schneider, G.E., and DeVos, R., "Nondimensional Analysis for the Heat Transport Capability of Axially-Grooved Heat Pipes Including Liquid/Vapor Interaction," *AIAA Paper* No. 80-0214, 1980.

5. Gao, M., Cao, Y., Beam, J. E., and Donovan, B., "Structural Optimization of Axially Grooved Flat Miniature Heat Pipes", *Enhanced Heat Transfer*, Vol. 7, pp361-369, 2000.
6. Gao, M., Cao, Y., Jones, W. K., and Zampino, M. A., "Ceramic Heat Pipes and Liquid Charging Methods", *Proceedings of the ASME, Heat Transfer Division*, Vol.4, pp. 429-434, 2000.
7. Cao, Y., Gao, M., and Pinilla, E., "Fabrication and test of a filling station for micro/miniature devices", *Electrochemical Technologies Conversion Technologies Thermal Management Proceedings of the Intersociety Energy Conversion Engineering Conference v 2*, IEEE, Piscataway, NJ, 97CB36203. pp. 1509-1513, 1997.
8. Plesch, D., Bier, W., Seidel, D. and Achubert, K., 1991, "Ministure heat pipes for heat removal from microelectronic circuits". DSC 32, *Micromechanical Sensors, Actuators, and Systems*, ASME.
9. Badran, B., Gerner, F. M., Ramada, P., Henderson, T., and Baker, K. W., 1997, "Experimental results for low-temperature silicon micromachined micro heat pipe array using water and methanol as working fluids", *Experimental Heat Transfer*, Oct.
10. Duncan, A.B., and Peterson, G. P., 1995, "Charge optimization of triangular shaped micro heat pipes", *AIAA J, Thermophys. Heat Transfer*, 9, pp.365-367.
11. Benson, D. A., Burchett, S. N., Kravitz, S. H., Tigges, C. P., Schmidt, C., and Robino, C. V., "Kovar micro heat pipe substrates for microelectronic cooling", *Report of Sandia National Laboratories*, 1999.
12. Cao Y., Gao M., Beam J. E., and Donovan B., "Experiments and Analysis of Flat Miniature heat Pipes", *AIAA Journal of Thermophysics and Heat Transfer*, 11(2), April-June, 1997.

## NOMENCLATURE

Symbol	Description
A	cross-sectional area, $m^2$
$D_g$	groove depth, m
$D_h$	hydraulic diameter, m
F	frictional coefficient
$h_{fg}$	latent heat of vaporization, J/kg
$L_{eff}$	effective heat pipe length, m
K	wick permeability, $m^2$
N	number of grooves
$Q_{cap}$	capillary limit, W
Re	Reynold's Number
$R_h$	hydraulic radius, $D_h/2$
$s_g$	groove spacing, m
$t_v$	vapor space height, m
w	width, m

### Greek Symbols

Symbol	Description
$\alpha$	$t_v/W$
$\mu$	viscosity, kg/(m-s)
$\rho$	density, $kg/m^3$

$\sigma$	liquid surface tension, N/m
$\phi$	wick porosity

### **Subscripts**

Symbol	Description
$g$	groove
$l$	liquid
$v$	vapor

### **Acronyms**

Acronym	Description
FIU	Florida International University
HTCC	High Temperature Cofired Ceramic
LTCC	Low Temperature Cofired Ceramic
MCM	Multi-Chip Module
OD	Outside Diameter